

1 **Exergoeconomic Analysis of an Absorption Refrigeration and Natural**
2
3
4 **Gas-Fueled Diesel Power Generator Cogeneration System**

5
6
7
8
9
10 **4 Felipe Raúl Ponce Arrieta***

11
12 Pontifical Catholic University of Minas Gerais, Department of Mechanical Engineering
13
14
15 Av. Dom José Gaspar, 500 - 30535-901 – Belo Horizonte – MG - Brazil
16
17 Phone: +55-31-9614-5380 - Fax: +55-31-3319-4910 - E-mail: felipe.ponce@pucminas.br
18
19

20
21 **8 José Ricardo Sodré**

22
23 Pontifical Catholic University of Minas Gerais, Department of Mechanical Engineering
24
25
26 Av. Dom José Gaspar, 500 - 30535-901 – Belo Horizonte – MG - Brazil
27
28 Phone: +55-31-3319-4911 - Fax: +55-31-3319-4910 - E-mail: ricardo@pucminas.br
29
30

31 **12 Mario David Mateus Herrera**

32
33 Pontifical Catholic University of Minas Gerais, Department of Mechanical Engineering
34
35
36 Av. Dom José Gaspar, 500 - 30535-901 – Belo Horizonte – MG - Brazil
37
38
39 Phone: +55-31-3319-4910 - E-mail: mario_mateus_h@hotmail.com
40
41

42 **16 Paola Helena Barros Zárante**

43
44 Pontifical Catholic University of Minas Gerais, Department of Mechanical Engineering
45
46
47 Av. Dom José Gaspar, 500 - 30535-901 – Belo Horizonte – MG - Brazil
48
49
50 Phone: +55-31-9670-0290 - E-mail: paolabarros@hotmail.com
51

52
53 **20 * corresponding author**
54
55
56
57
58
59
60

1 21 **ABSTRACT**

2
3 22

4
5
6 23 This work presents a thermoeconomic analysis of a cogeneration system using
7
8 24 the exhaust gas from a natural gas-fueled diesel power generator as heat source for an
9
10
11 25 ammonia-water absorption refrigeration system. The purpose of the analysis is to obtain
12
13 26 both unit exergetic and exergoeconomic costs of the cogeneration system at different
14
15
16 27 load conditions and replacement rates of diesel oil by natural gas. A thermodynamic
17
18 28 model of the absorption chiller was developed using the Engineering Equation Solver
19
20 29 (EES) software to simulate the exergetic and exergoeconomic cogeneration costs. The
21
22 30 data entry for the simulation model included available experimental data from a dual-
23
24
25 31 fuel diesel power generator operating with replacement rates of diesel oil by natural gas
26
27
28 32 of 25%, 50% and 75%, and varying engine load from 10 kW to 30 kW. Other required
29
30 33 data was calculations using the GateCycle software, from the available experimental
31
32
33 34 data. The results show that, in general, the cogeneration cold unit exergetic and
34
35 35 exergoeconomic costs increases with increasing engine load and decreases with
36
37
38 36 increasing replacement rate of diesel oil by natural gas under the conditions
39
40 37 investigated. Operating with 3/4 of the rated engine power and replacing 50% of diesel
41
42 38 oil by natural gas, the exergoeconomic cost of the produced power is increased by 75%,
43
44
45 39 and the exergoeconomic cost of the produced cold is decreased by 17%. The electric
46
47 40 power unit exergetic and exergoeconomic costs indicate that the replacement of diesel
48
49
50 41 oil by natural gas is feasible in the present considerations for engine operation at
51
52 42 medium and high loads.

53
54
55 43
56
57
58
59
60

1 44 Keywords: natural gas; cogeneration; absorption refrigeration; power generation;
2
3 45 exergoeconomic analysis.
4
5
6
7
8
9
10
11
12
13
14
15
16
17
18
19
20
21
22
23
24
25
26
27
28
29
30
31
32
33
34
35
36
37
38
39
40
41
42
43
44
45
46
47
48
49
50
51
52
53
54
55
56
57
58
59
60
61
62
63
64
65

1 70 another work, it was found that the highest performance of an ammonia-water
2
3 71 absorption refrigeration cycle integrated with a marine diesel engine was obtained at
4
5
6 72 high generator and evaporator temperatures, and low condenser and absorber
7
8 73 temperatures [11].
9

10
11 74 An experimental investigation of a solar thermal powered ammonia-water
12
13 75 absorption refrigeration system indicated a chiller COP of 0.69 and cooling capacity of 10.1
14
15
16 76 kW, with generator inlet temperature of 114°C, condenser/absorber inlet temperature of
17
18 77 23°C, and evaporator outlet temperature of -2°C [12]. A hybrid absorption-compression
19
20 78 refrigeration powered by mid-temperature waste heat reached a COP of 0.71, which is
21
22
23 79 about 42% higher than that of a conventional ammonia-water absorption refrigeration
24
25 80 system [13]. An energetic and exergetic study of a 10 RT (35.17 kW), single effect, indirect
26
27
28 81 heated LiBr absorption chiller coupled to a 30 kW microturbine, cooling tower and a heat
29
30 82 exchanger, using the Engineering Equation Solver (EES) software to evaluate the influence
31
32
33 83 of the system parameters, reports a COP around 0.7 for microturbine operation between
34
35 84 80% and 100% of the rated load [14]. The COP of a double effect LiBr absorption chiller,
36
37
38 85 of 1.411, was higher than that of a single effect chiller, of 0.809, both operating with waste
39
40 86 heat recovery from a boiler flue gas [15]. The exergetic efficiency of the absorption systems
41
42 87 decreased with increasing flue gas temperature due to the rise of irreversibility in the low
43
44
45 88 pressure generator.
46

47 89 A thermoeconomic evaluation is important to improve absorption refrigeration
48
49
50 90 systems, as they are less efficient than vapor compression systems [16,17]. An
51
52 91 exergoeconomic analysis was performed for three classes of double-effect, lithium
53
54
55 92 bromide-water absorption refrigeration systems, showing that lower investment costs
56
57 93 are attained when the temperatures of the high-pressure generator and the evaporator are
58

1 94 high, the condenser temperature is low [16]. The exergoeconomic analysis of series flow
2
3 95 double effect and combined ejector-double effect lithium bromide-water absorption
4
5
6 96 refrigeration systems pointed out that, with similar operating conditions, the overall
7
8 97 system investment cost and the product cost flow rate are lower for the combined cycle
9
10
11 98 [17]. In another work, an exergoeconomic analysis of a 5 kW ammonia-water
12
13 99 refrigeration cycle with hybrid storage system, with the solution properties determined
14
15
16 100 by the EES software, showed that the system overall exergetic efficiency tends to a
17
18 101 constant at temperatures higher than 120°C, and decreases with evaporator temperature
19
20 102 lower than -15°C [18]. A thermoeconomic analysis performed for an absorption
21
22
23 103 refrigeration system using the exhaust gas of a hydrogen-fueled diesel engine as energy
24
25 104 source showed that engine combustion is the process with the highest exergy
26
27
28 105 destruction, and that it is feasible to operate the system at intermediate and high engine
29
30 106 loads [19].

31
32
33 107 This work presents a thermoeconomic analysis of a cogeneration system
34
35 108 consisted by a direct heated, single effect, ammonia-water absorption refrigeration
36
37
38 109 system using as heat source the exhaust gas from a diesel power generator fueled by
39
40 110 diesel oil and natural gas. The exergetic and exergoeconomic analysis uses a similar
41
42 111 approach as that applied by [19]. The main aim is to study the performance parameters
43
44
45 112 of the cogeneration system and to get both exergetic and exergoeconomic costs of
46
47 113 power and cold production at different engine load conditions and replacement rates of
48
49
50 114 diesel oil by natural gas. The absorption refrigeration system was modeled in the EES
51
52 115 software, using as input data the experimental data available from a production,
53
54
55 116 stationary diesel engine operating in dual fuel mode with replacement rates of diesel oil
56
57 117 by natural gas of 25%, 50% and 75%, under variable load [20]. The experimental data
58

1 118 available was also used by the GateCycle software to calculate unmeasured exhaust gas
2
3 119 properties required by the absorption chiller simulation model.
4
5

6 120 Natural gas has clean burn features and produces lower levels of most pollutant
7
8 121 emissions components, compared with gasoline and diesel oil [21-27]. In dual fuel
9
10 122 operation with diesel oil, natural gas combustion increases heat release by about 27-
11
12 123 30%, compared to operation with diesel oil as a single fuel [28]. This results in reduced
13
14 124 specific fuel consumption, especially at high engine load and intake air temperature [21-
15
16 125 23,29]. The use of different replacement rates of diesel fuel by natural gas affects
17
18 126 combustion duration and exhaust gas temperature and, therefore, the energy available to
19
20 127 be used by the absorption refrigeration system [20]. In this work, the replacement rates
21
22 128 chosen allows for the analysis of a broad range of engine operation with equal
23
24 129 increments of natural gas in the fuel. The investigation of a cogeneration system
25
26 130 composed by an absorption refrigeration system and a diesel power generator operating
27
28 131 with different replacement rates of diesel oil by natural gas finds no resemblance to
29
30 132 previous works [5,9,11,14].
31
32
33
34
35
36
37

38 133 **2. DESCRIPTION OF THE COGENERATION SYSTEM**

39
40 134

41
42 135
43
44
45 136 A schematics of the absorption refrigeration system simulation coupled with the
46
47 137 diesel power generator is shown in Fig. 1. The power generation unit features a four-
48
49 138 stroke, four-cylinders, naturally aspirated diesel engine, with direct fuel injection and 44
50
51 139 kW rated power at 1800 rpm. The engine has a compression ratio of 17:1, 3.922 L total
52
53 140 displacement, 120 mm bore and 120 mm stroke. The simulated absorption refrigeration
54
55 141 system is direct heating, single effect, with ~17 kW (~ 4.8 TR) of capacity and COP ~
56
57
58

1 142 0.6. The refrigeration system has a generator containing a double rectifying column with
2
3 143 a second heat exchanger and a binary mixture as a combination of refrigerant and
4
5
6 144 absorbent. Ammonia is the refrigerant and water is the absorbent.
7

8 145 A strong liquid solution with a large concentration of ammonia refrigerant leaves
9
10
11 146 the absorber at state 1 and is pumped to the condensing pressure, being preheated in the
12
13 147 heat exchanger to reduce heating at state 3 (Fig. 1). The heated strong solution enters
14
15
16 148 into the generator, which produces a weak liquid solution with low concentration of
17
18 149 ammonia refrigerant at the bottom, at state 4, and nearly pure ammonia (99.98%) vapor
19
20 150 at the top, at state 7. The weak solution enters the heat exchanger and flows through the
21
22
23 151 pressure reducing valve to enter the absorber. The strong solution is sent to the
24
25 152 condenser at state 7, then it condenses to sub-cooled liquid at state 8. The liquid enters
26
27
28 153 the heat exchanger to cool at state 9 and, then, it enters the expansion valve. The
29
30 154 ammonia leaving the expansion valve at state 10 enters the evaporator, where the liquid
31
32
33 155 phase vaporizes to absorb the refrigerant load in the system. The refrigerant is further
34
35 156 heated in the heat exchanger prior to being absorbed in the weak-liquid solution in the
36
37
38 157 absorber at state 12, and, then, it returns to state 1, thus restarting the refrigeration cycle.
39

40 158

41 159 **3. METHODOLOGY**

42 160

43
44
45
46
47 161 Figure 2 presents the stages used in the methodology of the cogeneration system
48
49
50 162 simulation: processing of the available data from experimental engine testing and
51
52 163 calculation of exhaust gas related parameters by the GateCycle software, and simulation
53
54
55 164 of the absorption refrigeration system and exergoeconomic analysis in the EES
56
57 165 software. The experimental data and the results from the GateCycle software are used as
58
59
60

1 166 input data for the EES software, and both softwares operate independently. The
2
3 167 simulation does not aim to optimize the performance of the combined cogeneration
4
5
6 168 system, but to produce the necessary information for an exergetic and exergoeconomic
7
8 169 analysis of system operation with different replacement rates of diesel fuel by natural
9
10
11 170 gas.

12
13 171 The experimental data was available from tests in a production, four-stroke,
14
15
16 172 four-cylinder, stationary diesel engine, model MWM D229-4, of 44 kW rated power
17
18 173 operating at 1800 rev/min, compression ratio 17:1 and direct diesel fuel injection (Tab.
19
20 174 1) [29]. For all tested operating conditions, the exhaust gas temperature at the outlet of
21
22
23 175 the refrigeration system generator was $58^{\circ}\text{C} \pm 6^{\circ}\text{C}$ lower than the inlet gas temperature.
24
25 176 The engine was operated with varying load from 10 kW to 30 kW and with replacement
26
27
28 177 rates of diesel oil by natural gas of 0%, 25%, 50% and 75% on energy basis. During the
29
30 178 tests, the load power range was limited to 30 kW and the natural gas concentration was
31
32
33 179 limited to 75% due to engine instability to operate with natural gas at higher loads and
34
35 180 concentrations without major modifications. Additional details of the tests, including
36
37
38 181 the uncertainties of the results, can be found in Ref [29].

39
40 182 The GateCycle software uses the experimental data from the engine tests
41
42 183 varying the load applied and the replacement rate of diesel fuel by natural gas (Tab. 1)
43
44
45 184 to calculate unmeasured parameters by bivariate interpolation. The motivation to use the
46
47 185 GateCycle software was the possibility to use its internal libraries and adequately
48
49
50 186 estimate the exhaust gas properties required by the simulation model of the absorption
51
52 187 refrigeration system.

53
54
55 188 The compositions of natural gas and diesel oil are presented in Table 2. For
56
57 189 calculation of the total exergy of air, exhaust gas, diesel oil and natural gas, it was
58

1 190 considered steady state condition, negligible pressure drop and ambient at 30°C, 101.32
2
3 191 kPa [20]. The exergetic efficiency of the diesel power generator () is calculated by [19]:
4
5

6 192
7
8
9
10
11
12
13 193
14
15 194 Where is the output power from the diesel power generator (kW), is
16
17
18 195 the total exergy supplied with the fuel (kW), is the diesel oil mass flow rate
19
20 196 (kg/s), is the natural gas mass flow rate (kg/s), is the diesel oil specific exergy
21
22
23 197 (Table 2) (kJ/kg), and is the natural gas specific exergy (Table 2) (kJ/kg).
24

25 198 The simulation model of the absorption refrigeration system, developed in the
26
27
28 199 EES software, was validated against experimental data available from a commercial,
29
30 200 Consul CQG22D model ammonia-water absorption refrigerator used for domestic
31
32 201 application, of 215 L internal volume [2,31]. The refrigerator COP was kept nearly
33
34
35 202 constant, varying from 0.60 to 0.61, for all engine load range investigated. The
36
37 203 thermodynamic simulation of each system component calculates mass, energy, entropy
38
39
40 204 and exergy balances at steady state condition and neglecting pressure drop. The
41
42 205 exergetic efficiencies of the ammonia-water absorption refrigeration system () and
43
44
45 206 the system generator () are calculated as [19]:
46

47 207
48
49
50
51
52
53
54 208
55
56

1 209
 2
 3
 4 210 Where and are the total exergies of the produced cold and the engine
 5
 6 211 exhaust gas, respectively (kW), and is the power consumed by the solution pump
 7
 8
 9 212 (kW). , , are pure ammonia specific exergies at the state 7, evaporator
 10
 11 213 inlet and evaporator outlet, respectively (kJ/kg), and is the exhaust gas specific
 12
 13
 14 214 exergy variation from the generator inlet to outlet (kJ/kg). and are the binary
 15
 16 215 solution specific exergies at the states 3 and 4, respectively (kJ/kg). and are the
 17
 18 216 binary solution specific enthalpies at the pump inlet and outlet, respectively, in kJ/kg.
 19
 20
 21 217 is the exhaust gas flow rate at the generator inlet (kg/s); and are pure
 22
 23 218 ammonia flow rates at the evaporator and state 7, respectively (kg/s). and are the
 24
 25
 26 219 binary solution flow rates at states 3 and 4, respectively (kg/s).
 27
 28 220 Other results from the third stage of the simulation include component
 29
 30
 31 221 irreversibilities, generator efficiency, heat transfer in the condenser, evaporator,
 32
 33 222 absorber and heat exchanger, pump power, COP, and the thermodynamic properties
 34
 35
 36 223 used in the exergoeconomic analysis (stage 5 in Fig. 2). The exergoeconomic analysis
 37
 38 224 refers to the exergetic costs of system operation according to the physical structure of
 39
 40 225 the cogeneration system (Fig. 1), using the streams thermodynamic properties and
 41
 42
 43 226 component parameters that were computed in the previous stages (Fig. 2). For the
 44
 45 227 exergoeconomic analysis, the unit exergetic cost at the cogeneration system inlet was
 46
 47
 48 228 assumed as 1, the exergetic cost balance was applied for components and junctions, and
 49
 50 229 the costs distribution in the bifurcations was performed proportionally to the exergy.
 51
 52
 53 230 Additionally, the negentropy was considered to be generated by dissipative equipment,
 54
 55 231 such as the condenser and absorber, and the exhaust gas from the diesel power generator
 56
 57
 58 232 was taken as waste when assigning the costs.

Table 3 presents the fuel-product definition for each component of the cogeneration system, based on which the cogeneration plant productive structure was built (Fig. 3). Figure 3 shows that the negentropy () related to heat dissipation in the condenser is located in the generator, heat exchanger, evaporator and expansion valve (streams 39 to 42), and related to heat dissipation in the absorber is located in the pressure reducing valve, generator, solution heat exchanger and solution pump (streams 35 to 38). The negentropy distribution adopted was based on the criteria that some components work with nearly pure ammonia (heat exchanger, expansion valve and evaporator) while others use ammonia-water solution (solution heat exchanger, pressure reducing valve and solution pump) or both (generator). For the generator, two negentropy streams were located (36 and 39) because it works with two fluid types: nearly pure ammonia (flow 7 in Fig. 1) and ammonia-water solution (flows 3 and 4 in Fig. 1).

The diesel engine negentropy is due to dissipation of the chemical exergy of the exhaust gas flow to the ambient (ambient product in Tab. 3 and stream 47 in Fig. 3). From the 50 streams presented in Fig. 3 and the assumptions mentioned before, 50 equations were written in the EES software to compute the unit exergetic cost for each stream, with the aim to calculate the unit exergetic cost (, in dimensionless form) and the specific exergoeconomic cost () of each stream in the productive structure. The main calculated costs were the net electrical power (, in US\$/kW.h) and cold produced (, in US\$/RT.h, 1 RT = 3.517 kW) by the system at the different loads and fuel replacement rates simulated. The specific costs are calculated by the following equations [19]:

1
2
3
4
5 257
6
7
8
9
10

11 258
12
13

14 259 Where \dot{C} is the total stream exergetic cost (kW), \dot{E} is the total stream exergy
15
16 260 (kW), η is the exergetic efficiency (dimensionless), and \dot{C}_{ex} is the stream
17
18 261 exergoeconomic cost (US\$/h).
19
20

21 262 The exergoeconomic costs for each stream in Fig. 3 are calculated from the
22
23 263 exergetic unit costs. The exergoeconomic costs are due to fuel prices, taking into
24
25 264 account the initial investment, maintenance and external valorization. The diesel oil and
26
27 265 natural gas prices considered in the calculations were 0.2 US\$/L and 0.5465 US\$/m³,
28
29 266 respectively. These are commercialization prices for thermal power generation
30
31 267 established by the Brazilian Ministry of Finance [32]. The calculation of the external
32
33 268 valorization was based on Ref. [33], and it includes an investment cost of US\$
34
35 269 13,950.00 for the diesel power generator and US\$ 13,167.00 for the absorption
36
37 270 refrigeration system. Further details on the exergoeconomic analysis are available in
38
39 271 Ref. [20].
40
41
42
43
44
45

46 272
47

48 273 4. RESULTS AND DISCUSSION

49
50 274

51
52 275 Figure 4 shows that the engine exergetic efficiency increased with increasing
53
54 276 load power. This trend is explained because, at low loads, a high fraction of the power
55
56 277 produced is used to overcome friction losses. At partial load, fluid flows, mixing, heat
57
58
59
60

1 278 transfer and combustion processes increase the specific entropy generation, thus
2
3 279 reducing the exergetic efficiency. It is also observed that, with increasing diesel oil
4
5
6 280 replacement by natural gas at any load, the engine exergetic efficiency is enhanced due
7
8 281 to improved combustion. The increase of natural gas fraction in the fuel also increases
9
10
11 282 the pre-mixed combustion phase, which is a process more efficient than diffusive
12
13 283 combustion.

14
15
16 284 In Fig. 5, it is observed that the exergetic efficiency of the refrigeration system
17
18 285 tends to decrease with increasing load, due to rise of heat transfer and irreversibility in
19
20 286 the refrigeration system. When the engine load increases, the exhaust gas mass flowrate
21
22
23 287 and temperature are also increased (Tab. 1). Thus, more heat is transferred to the
24
25 288 refrigeration system, and the heat transfer process in the refrigeration system regenerator
26
27
28 289 occurs with a higher temperature difference. For those reasons, both entropy generation
29
30 290 and irreversibility are increased, causing a decrease of the exergetic efficiency of the
31
32
33 291 absorption refrigeration system. Increasing the replacement rate of diesel oil by natural
34
35 292 gas until 50% decreases the exhaust gas temperature (Tab. 1), which can improve the
36
37
38 293 exergetic efficiency.

39
40 294 Figure 6 shows a tendency of reducing generator exergetic efficiency when the
41
42 295 engine load is increased, similarly to what was observed for the absorption refrigeration
43
44
45 296 system (Fig. 5). This means that the exergetic efficiency of the absorption refrigeration
46
47 297 system is strongly influenced by the generator exergetic efficiency. The generator
48
49
50 298 exergetic efficiency decreases with increasing engine load because of higher entropy
51
52 299 generation (or irreversibility) caused by high heat transfer rate and temperature
53
54
55 300 difference between the engine exhaust gas and the refrigeration system working fluid.

1 301 Figure 7 shows that the produced cold unit exergetic cost is increased with
2
3 302 increasing engine load, and is decreased with increasing replacement rate of diesel oil
4
5
6 303 by natural gas. This means that more exergy is necessary to supply the refrigeration
7
8 304 system for each unit of produced cold when increasing engine load. In Fig. 8, it is
9
10
11 305 observed that the produced power unit exergetic cost decreases for medium and high
12
13 306 loads while, for low and partial loads, the cost is higher. This means that less exergy is
14
15
16 307 necessary to supply the engine for each unit of the produced power when increasing
17
18 308 engine load or, in other words, it is more interesting to operate the engine at high loads
19
20 309 to reduce the power generation cost. Increasing the replacement rate of diesel oil by
21
22
23 310 natural gas also decreases unit exergetic cost of power generation.
24

25 311 Figure 9 shows that the exergoeconomic cost of the cogenerated cold is
26
27
28 312 increased with increasing load and decreased with increasing replacement rate of diesel
29
30 313 oil by natural gas. The decrease of the exergetic efficiency of the absorption
31
32
33 314 refrigeration system with increasing engine load (Fig. 5) increases the irreversibility
34
35 315 and, thus, the final cost of the cogenerated cold. On the other hand, the exergetic
36
37
38 316 efficiency of the absorption refrigeration system is increased with increasing
39
40 317 replacement of diesel oil by natural gas (Fig. 5), having a positive effect on the
41
42 318 exergoeconomic cost of the cogenerated cold (Fig. 9).
43
44

45 319 The variation of the exergoeconomic cost of electrical power production is
46
47 320 shown by Fig. 10. Unlike cold cogeneration, in this case the trend of decreasing cost
48
49
50 321 with increasing load is due to the increase of the engine exergetic efficiency (Fig. 4),
51
52 322 which reduces the irreversibility of the power system. Increasing the replacement rate of
53
54
55 323 diesel oil by natural gas increases the exergoeconomic cost of power production (Fig.
56
57 324 10). Considering the prices of residential rates with taxes, both the use of diesel oil as a
58

1 325 single fuel or partially replacing it by natural gas can be competitive in the depicted
2
3 326 scenario if the cost of electrical power is lower than the existing rate with taxes. When
4
5
6 327 natural gas is used, the exergoeconomic cost of the produced power is below the
7
8 328 existing rate with taxes only at intermediate and high loads. The gaseous fuel cost has a
9
10
11 329 strong influence on the calculated results, playing a major role to make the cogeneration
12
13 330 system economically viable.

14
15
16 331 From comparison of the results of the present work with those when hydrogen
17
18 332 was used as fuel in similar conditions [19], the same trends were observed for the
19
20 333 produced cold and power exergoeconomic costs (Figs. 9 and 10). Nevertheless,
21
22
23 334 considering the replacement rate of 50%, the reduction of the produced cold
24
25 335 exergoeconomic cost is of about 26% when hydrogen replaces diesel oil [19], while,
26
27
28 336 using natural gas instead, the reduction is of around 17% (Fig. 9). When analyzing the
29
30 337 produced power exergoeconomic cost, the use of hydrogen is more viable for a slightly
31
32
33 338 larger range of load power [19]. However, natural gas allows for a larger replacement
34
35 339 rate of diesel oil, up to 75% without major engine modification, while the maximum
36
37
38 340 replacement rate of diesel oil by hydrogen was 50% [19].

39 341

40 342 **5. CONCLUSIONS**

41
42 343

43
44
45 344 From the results obtained, the following conclusions can be drawn:

- 46
47 345 – Increasing engine load reduces entropy generation and irreversibility in the engine
48
49
50 346 and increases entropy generation and irreversibility in the absorption refrigeration
51
52
53 347 system;

1 348 – Increasing the replacement rate of diesel oil by natural gas decreases entropy
2
3 349 generation and irreversibility in both the engine and the absorption refrigeration
4
5 350 system;
6
7
8 351 – The cogeneration cold unit exergetic cost and exergoeconomic cost increase with
9
10 352 engine load due to an increase of exergy destruction in the absorption refrigeration
11
12 353 system mainly by the reduction of the exergetic efficiency in the generator of the
13
14 354 refrigeration system.
15
16 355 – The cogeneration cold unit exergetic cost and exergoeconomic cost decrease with
17
18 356 increasing replacement rates of diesel oil by natural gas;
19
20 357 – The electric power unit exergetic cost and exergoeconomic cost decrease with
21
22 358 increasing engine load and diesel oil replacement by natural gas rise, being viable
23
24 359 in the economic scenario considered if the engine is operated at medium and high
25
26 360 loads;
27
28 361 – In comparison with diesel fuel replacement by hydrogen, natural gas provides lower
29
30 362 decrease of the exergoeconomic cost of cold production, but allows for a larger
31
32 363 range of replacement rate without major engine modification.
33
34
35 364

365 **6. ACKNOWLEDGMENTS**

366 The authors thank CAPES, ANEEL/CEMIG GT-292 research project, CNPq
367 research project 304114/2013-8, and FAPEMIG research projects TEC PPM 0385-15
368 and TEC BPD 0309-13 for the financial support to this work.

370 **7. NOMENCLATURE**

371

1	372		Specific exergoeconomic cost, US\$/kW.h or US\$/RT.h
2			
3			
4	373		Exergoeconomic cost, US\$/h
5			
6	374	CO	Carbon monoxide
7			
8	375	COP	Coefficient of Performance
9			
10			
11	376	EES	Engineering Equation Solver
12			
13	377		Specific exergy, kJ/kg
14			
15			
16	378		Total exergy, kW
17			
18	379		Total exergy cost, kW
19			
20			
21	380	h	Binary solution specific enthalpy, kJ/kg
22			
23	381		Unit exergetic cost, kW/kW
24			
25			
26	382	LiBr	Lithium Bromide
27			
28	383		Mass flowrate, kg/s
29			
30			
31	384	NG	Natural Gas
32			
33	385	NMHC	Non-Methane unburned hydrocarbons
34			
35			
36	386	NO _x	Oxides of nitrogen
37			
38	387	SPECO	Specific Exergy Costing
39			
40			
41	388		Power, kW
42			
43	389		
44			
45	390		<i>Greek letters</i>
46			
47			
48	391		Variation or difference
49			
50	392		Efficiency
51			
52			
53	393		
54			
55	394		<i>Subscripts</i>
56			
57			
58	395	1, 2,...	Flow number (Fig. 1) or stream number (Fig. 5)
59			
60			
61			
62			

1	396	Absorber
2		
3		
4	397	Absorption Refrigeration System
5		
6	398	Cold
7		
8	399	Chemical
9		
10		
11	400	Condenser
12		
13	401	Diesel oil
14		
15		
16	402	Diesel Engine
17		
18	403	Electric power
19		
20		
21	404	Expansion Valve
22		
23	405	Evaporator
24		
25		
26	406	Diesel oil and natural gas blend
27		
28	407	Exhaust gas
29		
30		
31	408	Generator
32		
33	409	Heat Exchanger
34		
35		
36	410	Negentropy
37		
38	411	Natural Gas
39		
40		
41	412	Pressure Reduction Valve
42		
43	413	Refrigerant
44		
45		
46	414	Shaft power
47		
48	415	Solution Heat Exchanger
49		
50		
51	416	Solution pump
52		
53	417	
54		
55		
56	418	<i>Superscripts</i>
57		
58	419	Exergetic
59		
60		
61		
62		

1 420
2
3 421 **8. REFERENCES**
4
5
6 422
7

- 8 423 [1] F. Táboas, M. Bourouis, M. Vallès, Analysis of ammonia/water and ammonia/salt
9
10 mixture absorption cycles for refrigeration purposes in fishing ships. Applied
11 424 Thermal Engineering 66 (2014) 603-611.
12
13 425 <http://dx.doi.org/10.1016/j.applthermaleng.2014.02.065>
14
15
16 426
17
18 427 [2] A. Manzela, S. Hanriot, L. Cabezas-Gómez, J. Sodr . Using engine exhaust gas
19
20 428 energy source for an absorption refrigeration system. Applied Energy 87 (2012)
21
22 1141-1148. doi:10.1016/j.apenergy.2009.07.018
23
24
25 430 [3] A. Abusoglu, M. Kanoglu. Exergetic and thermoeconomic analyses of diesel engine
26
27 powered cogeneration: Part 1-Formulation. Applied Thermal Engineering 29
28 431 (2009) 234-241. doi:10.1016/j.applthermaleng.2008.02.025
29
30
31
32 433 [4] O. Balli, H. Aras, A. Hepbasli. Thermodynamic and thermoeconomic analyses of a
33
34 trigeneration (TRIGEN) system with a gas-diesel engine: Part I – Methodology.
35 434 Energy Conversion and Management 51 (2010) 2252-2259.
36
37
38 435
39
40 436 [5] O. Balli, H. Aras, A. Hepbasli. Thermodynamic and thermoeconomic analyses of a
41
42 437 trigeneration (TRIGEN) system with a gas-diesel engine: Part II – An application.
43
44 Energy Conversion and Management 51 (2010) 2260-2271.
45 438
46
47 439 doi:10.1016/j.enconman.2010.03.021
48
49
50 440 [6] J. Li, S. Xu, The performance of absorption – compression hybrid refrigeration
51
52 441 driven by waste heat and power from coach engine, Applied Thermal Engineering
53
54 61 (2013) 747–755. doi:10.1016/j.applthermaleng.2013.08.048
55 442
56
57
58
59
60
61
62
63
64
65

1 443 [7] M. Mostafavi, B. Agnew, Thermodynamic analysis of combined diesel engine and
2
3 444 absorption refrigeration unit-naturally aspirated diesel engine, Applied Thermal
4
5
6 445 Engineering 17 (1997) 471-478. doi:10.1016/S1359-4311(96)00036-1
7

8 446 [8] S. Jayasekara, S.K. Halamuge, A combined effect absorption chiller for enhanced
9
10
11 447 performance of combined cooling heating and power system, Applied Energy, 127
12
13 448 (2014) 239-248. doi:10.1016/j.apenergy.2014.04.035
14
15

16 449 [9] T.K. Gogoi, K. Talukdar, Exergy based parametric analysis of a combined reheat
17
18 450 regenerative thermal power plant and water-LiBr vapor absorption refrigeration
19
20 451 system, Energy Conversion and Management 83 (2014) 119-132.
21
22
23 452 doi:10.1016/j.enconman.2014.03.060
24

25 453 [10] A. Sencan, Performance of ammonia-water refrigeration systems using artificial
26
27
28 454 neural networks, Renew. Energy 32 (2007) 314-328.
29
30 455 doi:10.1016/j.renene.2006.01.003
31
32

33 456 [11] A. Ouadha, Y. El-Gotni, Integration of an ammonia-water absorption refrigeration
34
35 457 system with a marine Diesel engine: A thermodynamic study, Preced. Comput. Sci.
36
37
38 458 19 (2013) 754-761.
39

40 459 [12] S.A.M. Said, K. Spinder, M.A., El-Shaarawi, M.U. Siddiqui, F. Schmid, B.
41
42 460 Bierling, M.M.A. Khan, Design, construction and operation of a solar powered
43
44
45 461 ammonia-water absorption refrigeration system in Saudi Arabia, International
46
47 462 Journal of Refrigeration, 62 (2016) 222-231. doi:10.1016/j.ifrefrig.2015.10.026
48
49

50 463 [13] W. Han, L. Sun, D. Zheng, H. Jin, S. Ma, X. Jing, New hybrid absorption-
51
52 464 compression refrigeration system based on cascade use of mid-temperature waste
53
54
55 465 heat, Applied Energy 106 (2013) 383-390. doi:10.1016/j.apenergy.2013.01.067
56

1 466 [14] A.A.V. Ochoa, J.C.C. Dutra, J.R.G. Henríquez, J. Rohati, Energetic and exergetic
2
3 467 study 10 RT absorption chiller integrated into a microgeneration system, Energy
4
5
6 468 Conversion and Management 88 (2014) 545-553.
7
8 469 doi:10.1016/j.econman.2014.08.064
9
10
11 470 [15] K. Talukdor, T.K. Gogoi, Exergy analysis of a combined vapor power cycle and
12
13 471 boiler flue gas driven double effect water-LiBr absorption refrigeration system.
14
15
16 472 Energy Conversion and Management 108 (2016) 468-477.
17
18 473 doi:10.1016/j.econman.2015.11.020
19
20 474 [16] G. Farshi, S. Mahmoudi, M. Rosen, M. Yari, M. Amidpo, Exergoeconomic
21
22
23 475 analysis of double effect absorption refrigeration systems, Energy Conversion and
24
25 476 Management 65 (2013) 13-25. doi:10.1016/j.enconman.2012.07.019
26
27
28 477 [17] G. Farshi, S.M.S. Mahmoudi, M.A. Rosen, Exergoeconomic comparison of double
29
30 478 effect and combined ejector-double effect absorption systems, Applied Energy 103
31
32
33 479 (2013) 700-711. doi:10.1016/j.apenergy.2012.11.022
34
35 480 [18] F.R. Siddiqui, M.A.I. El-Shaarawi, S.A.M. Said, Exergo-economic analysis of a
36
37
38 481 solar driven hybrid storage absorption refrigeration cycle, Energy Conversion and
39
40 482 Management 80 (2014) 165-172. doi:10.1016/j.econman.2014.01.029
41
42 483 [19] M.D.M. Herrera, F.R.P. Arrieta, J.R. Sodr , Thermo-economic assessment of an
43
44
45 484 absorption refrigeration and hydrogen-fueled diesel power generator cogeneration
46
47 485 system, International Journal of Hydrogen Energy 39 (2014) 4590-4599.
48
49
50 486 doi:10.1016/j.ijhydene.2014.01.028
51
52 487 [20] M. Justino, M. Morais, A. Oliveira, O.S. Valente, J.R. Sodr , Fuel consumption of
53
54
55 488 a diesel engine fueled with hydrogen, natural gas and diesel blends. SAE Technical
56
57 489 Paper 2012; 2012-36-0107:1-6.
58

1 490 [21] R. Papagiannakis, D. Hountalas, Combustion and exhaust emission characteristics
2
3 491 of a dual fuel compression ignition engine operated with pilot Diesel fuel and
4
5
6 492 natural gas, *Energy Conversion and Management* 45 (2010) 2971–2987.
7
8 493 doi:10.1016/j.enconman.2004.01.013
9
10
11 494 [22] M. Karabektas, G. Ergen, M. Hosoz, The effects of using diethylether as additive
12
13 495 on the performance and emissions of a diesel engine fueled with CNG, *Fuel* 115
14
15
16 496 (2014) 855–860. doi:10.1016/j.fuel.2012.12.062
17
18 497 [23] R. Papagiannakis, P. Kotsiopoulos, T. Zannis, E. Yfantis, D. Hountalas, C.
19
20 498 Rakopoulos, Theoretical study of the effects of engine parameters on performance
21
22
23 499 and emissions of a pilot ignited natural gas diesel engine, *Energy* 35 (2010) 1129–
24
25 500 1138. doi:10.1016/j.energy.2009.06.006
26
27
28 501 [24] N. Mustafi, R. Raine, S. Verhelst, Combustion and emissions characteristic of a
29
30 502 dual fuel engine operated on alternative gaseous fuels, *Fuel* 109 (2013) 669–678.
31
32
33 503 doi:10.1016/j.fuel.2013.03.007
34
35 504 [25] S. Roy, A. K. Das, P. K. Bose, R. Banerjee, ANN metamodel assisted particle
36
37
38 505 swarm optimization of the performance-emission trade off characteristics of a
39
40 506 single cylinder CRDI engine CNG dual-fuel operation, *Journal of Natural Gas*
41
42 507 *Science and Engineering* 21 (2014) 1156-1162.
43
44
45 508 <http://dx.doi.org/j.jngse.2014.11.013>
46
47 509 [26] M. Shahraeni, S. Ahmed, K. Malek, B. Van Drimmelen, E. Kjeang, Life cycle
48
49
50 510 emissions and cost transportation systems: case study on diesel and natural gas for
51
52 511 light duty trucks in municipal fleet operations, *Journal of Natural Gas Science and*
53
54
55 512 *Engineering* 24 (2015) 26-34. <http://dx.doi.org/j.jngse.2015.03.009>

1 513 [27] J. Li, B. Wu, G. Mao, Research on the performance and emission characteristics of
2 514 the LNG-Diesel marine engine, *Journal of Natural Gas Science and Engineering* 27
3 515 (2015) 945-954. <http://dx.doi.org/j.jngse.2015.09.036>
4
5
6
7
8 516 [28] M. Mikulski, S. Wierzbicki, Numerical investigation of the impact of gas
9 517 composition on the combustion process in a dual-fuel compression-ignition engine,
10 518 *Journal of Natural Gas Science and Engineering* 31 (2016) 525-537.
11 519 <http://dx.doi.org/j.jngse.2016.03.074>
12
13
14
15
16
17
18 520 [29] K. Cheenkachorn, C. Poornipatpong, G. Ho, Performance and emissions of a
19 521 heavy-duty diesel engine fueled with diesel and LNG (liquid natural gas), *Energy*
20 522 53 (2013) 52–57. doi:10.1016/j.energy.2013.02.027
21
22
23
24
25 523 [30] M. Lozano, A. Valero. Calculation of exergy for substances of industrial
26 524 interesting. Dept. of Thermodynamics and Physic – Chemistry. ETSII. Zaragoza
27 525 University. Chemical Engineering magazine. March, 1986. (In Spanish).
28
29
30
31
32
33 526 [31] A. Rêgo, S. Hanriot, A. Oliveira, P. Brito, T. Rêgo. Automotive exhaust gas flow
34 527 control for an ammonia-water absorption refrigeration system. *Applied Thermal*
35 528 *Engineering* 64 (2014) 101-107. doi: 10.1016/j.applthermaleng.2013.12.018
36
37
38
39
40 529 [32] Brazilian Ministry of Finance. Table of maximum retail diesel oil prices. Available
41 530 in [www.fazenda.gov.br/portugues/legislacao /portarias_inter/2001/ anxport198.pdf](http://www.fazenda.gov.br/portugues/legislacao/portarias_inter/2001/anxport198.pdf).
42 531 Accessed in November 12th, 2015.
43
44
45
46
47 532 [33] H. Lima. Thermoeconomic analysis of an absorption refrigeration system with
48 533 LiBr-H₂O pair, 3rd European Congress on Economics and Management of Energy
49 534 in Industry, Lisbon, 2004.
50
51
52
53
54
55 535

1 536 **LIST OF TABLE CAPTIONS**
2
3
4 537
5
6
7 538 Table 1 – Experimental data from diesel power generator operating with natural gas
8
9 539 (NG) used in the simulation [20].
10
11
12 540 Table 2 – Natural gas and diesel data assumed for calculations.
13
14 541 Table 3 – Fuel – Product definition by component for the productive structure.
15
16
17 542
18
19
20
21
22
23
24
25
26
27
28
29
30
31
32
33
34
35
36
37
38
39
40
41
42
43
44
45
46
47
48
49
50
51
52
53
54
55
56
57
58
59
60
61
62
63
64
65

1	543	LIST OF FIGURE CAPTIONS
2		
3	544	
4		
5		
6	545	Figure 1 – Simplified schematics of the absorption refrigeration system coupled to the
7		
8	546	diesel power generator.
9		
10		
11	547	Figure 2 – Summary of the stages of the simulation model.
12		
13	548	Figure 3 – Cogeneration plant productive structure.
14		
15		
16	549	Figure 4 – Variation of engine exergetic efficiency with load power and natural gas
17		
18	550	concentration in the fuel.
19		
20	551	Figure 5 – Variation of absorption refrigeration system exergetic efficiency with engine
21		
22		
23	552	load power and natural gas concentration in the fuel.
24		
25	553	Figure 6 – Variation of generator exergetic efficiency with engine load power and
26		
27		
28	554	natural gas concentration in the fuel.
29		
30	555	Figure 7 – Variation of produced cold unit exergetic cost with engine load power and
31		
32		
33	556	natural gas concentration in the fuel.
34		
35	557	Figure 8 – Variation of produced power unit exergetic cost with engine load power and
36		
37		
38	558	natural gas concentration in the fuel.
39		
40	559	Figure 9 – Variation of produced cold exergoeconomic cost with engine load power and
41		
42	560	natural gas concentration in the fuel.
43		
44		
45	561	Figure 10 – Variation of produced power exergoeconomic cost with engine load power
46		
47	562	and natural gas concentration in the fuel.
48		
49		
50	563	
51		
52		

1 564
 2
 3 565
 4
 5 566
 6
 7
 8
 9
 10
 11
 12
 13
 14
 15
 16
 17
 18
 19
 20
 21
 22
 23
 24
 25 567
 26 568
 27
 28
 29
 30
 31
 32
 33
 34
 35
 36
 37
 38
 39
 40
 41
 42
 43
 44
 45
 46
 47
 48
 49
 50
 51
 52
 53
 54
 55
 56
 57
 58
 59
 60
 61
 62
 63
 64
 65

Table 1 – Experimental data from diesel power generator operating with natural gas (NG) used in the simulation [20].

ENGINE LOAD (kW)	100% DIESEL OIL			75% DIESEL OIL + 25% NG			50% DIESEL OIL + 50% NG			25% DIESEL OIL + 75% NG		
	EXHAUST	DIESEL	NG FLOW	EXHAUST	DIESEL	NG FLOW	EXHAUST	DIESEL	NG FLOW	EXHAUST	DIESEL	NG FLOW
	GAS	OIL	RATE	GAS	OIL	RATE	GAS	OIL	RATE	GAS	OIL	RATE
	TEMP (°C)	FLOW RATE (kg/h)	(kg/h)	TEMP (°C)	FLOW RATE (kg/h)	(kg/h)	TEMP (°C)	FLOW RATE (kg/h)	(kg/h)	TEMP (°C)	FLOW RATE (kg/h)	(kg/h)
0	143.01	1.91	-	145.00	1.86	-	138.63	1.93	-	148.41	1.32	-
10	224.09	3.37	0.786	220.00	2.94	0.786	214.64	2.88	1.573	223.64	2.33	2.359
20	324.17	5.17	1.171	312.00	4.50	1.171	307.11	4.10	2.341	313.99	3.48	3.511
30	447.79	7.15	1.627	430.00	6.32	1.627	419.85	5.80	3.254	420.20	5.23	4.880

Table 2 – Natural gas and diesel data assumed for calculations.

Natural gas		Diesel	
Component	Molar fraction	Component	Mass fraction
Nitrogen	0.015	Carbon	0.8670
Carbon Dioxide	0.007	Hydrogen	0.1271
Methane	0.871	Oxygen	0.0032
Ethane	0.078	Nitrogen	0,0000
Propane	0.029	Sulfur	0.0020
Hexane	0.000	Wet	0.0005
Hydrogen	0.000	Ash	0.0002
Lower Heating Value, kJ/kg	47451	Lower Heating Value, kJ/kg	43000
Specific exergy, kJ/kg	49243	Specific exergy, kJ/kg	42145

1 573 Table 3 – Fuel – Product definition by component for the productive structure.

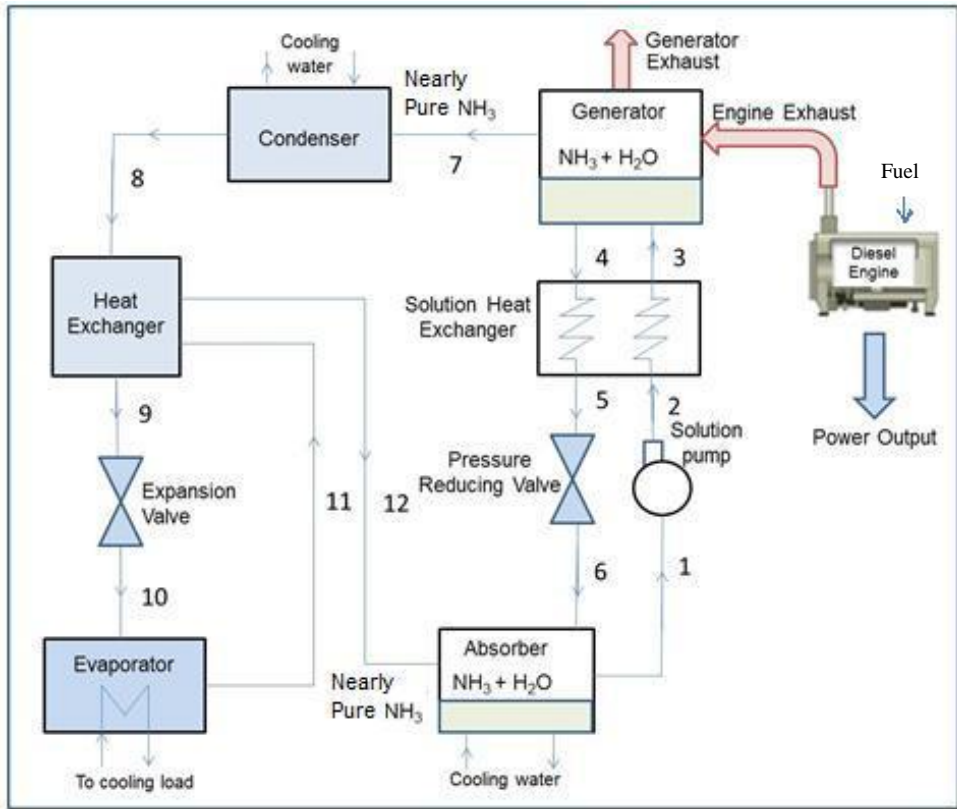
COMPONENT	FUEL	PRODUCT
Diesel engine		
Electric generator		
Ambient		
Generator		
Condenser		
Evaporator		
Absorber		
Solution pump		
Heat exchanger		
Solution heat exchanger		
Expansion valve		
Pressure reducing valve		

34 574

35
36 575

37
38
39
40
41
42
43
44
45
46
47
48
49
50
51
52
53
54
55
56
57
58
59
60
61
62
63
64
65

1
2
3
4
5
6
7
8
9
10
11
12
13
14
15
16
17
18
19
20
21
22
23
24
25
26
27
28
29
30
31
32
33
34
35
36
37
38
39
40
41
42
43
44
45
46
47
48
49
50
51
52
53
54
55
56
57
58
59
60
61
62
63
64
65



576

577 Figure 1 – Simplified schematics of the absorption refrigeration system coupled to the
578 diesel power generator.

579

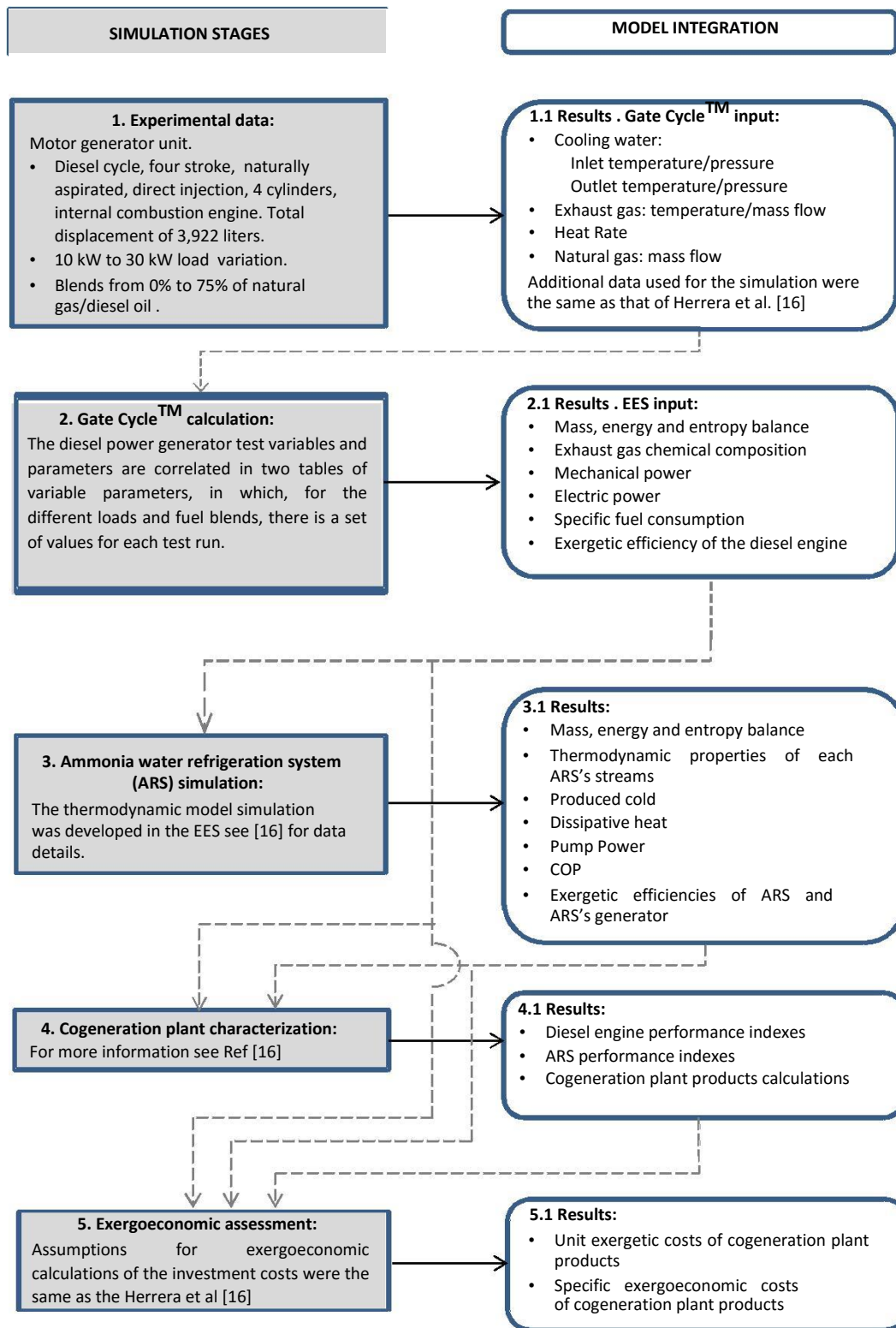


Figure 2 – Summary of the stages of the simulation model.

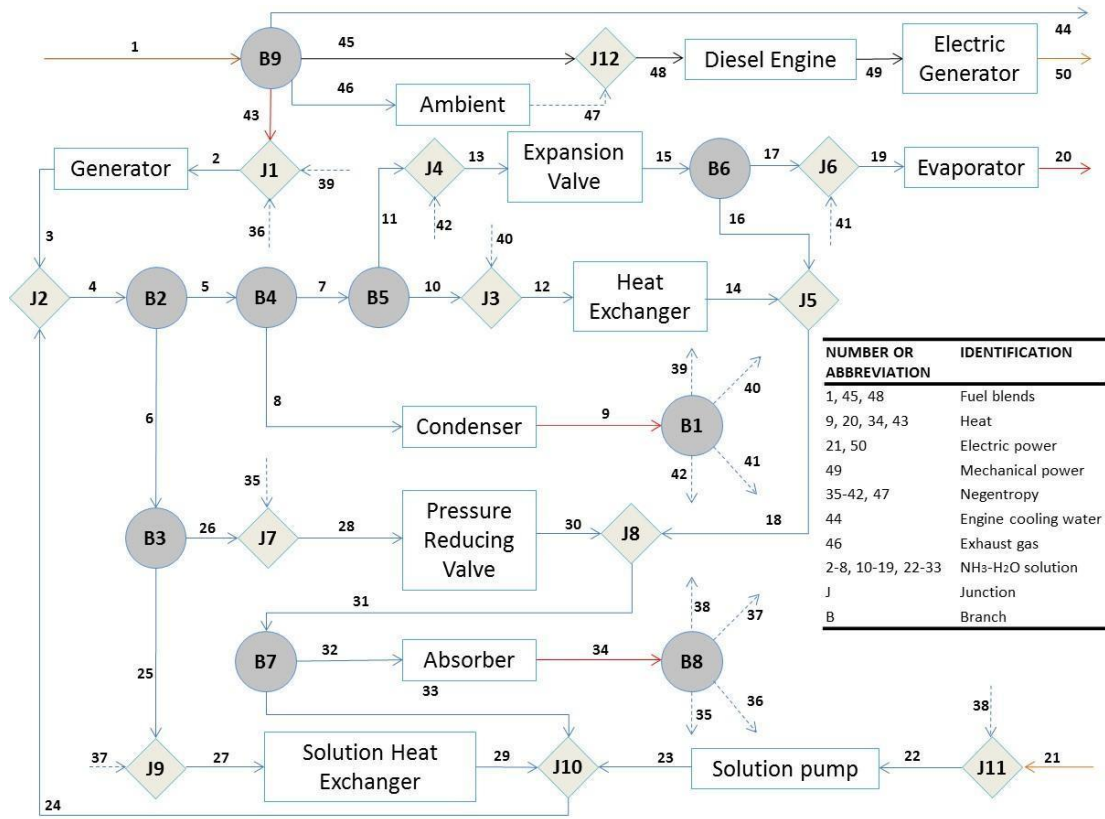
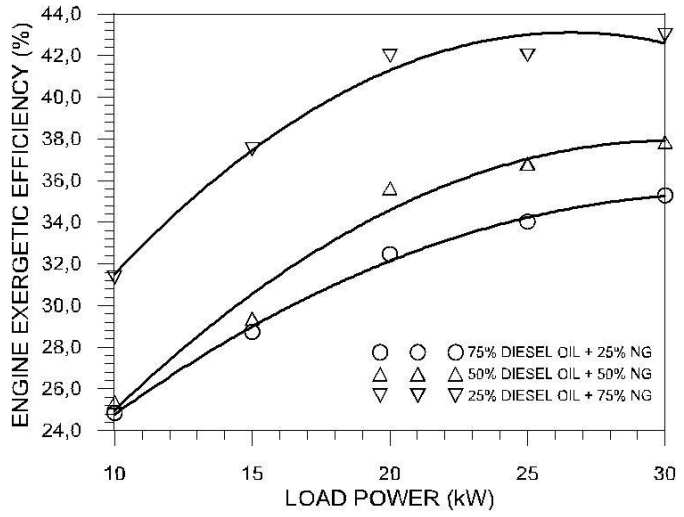


Figure 3 – Cogeneration plant productive structure.

1
2
3
4
5
6
7
8
9
10
11
12
13
14
15
16
17
18
19
20
21
22
23
24
25
26
27
28
29
30
31
32
33
34
35
36
37
38
39
40
41
42
43
44
45
46
47
48
49
50
51
52
53
54
55
56
57
58
59
60
61
62
63
64
65



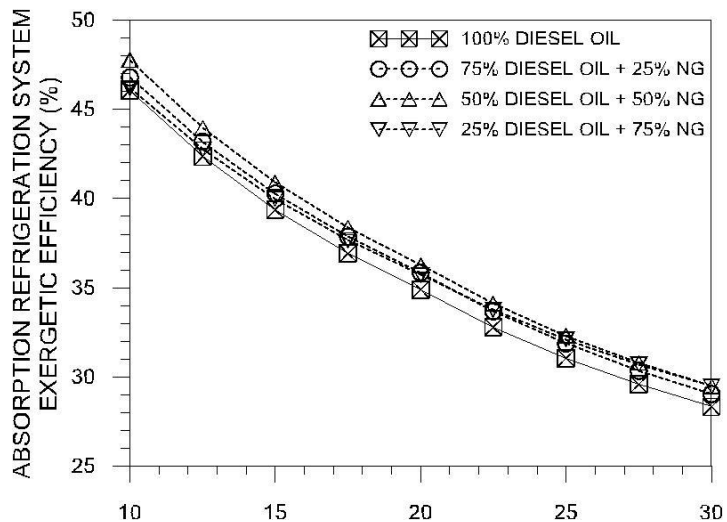
586

587

588

589

Figure 4 – Variation of engine exergetic efficiency with load power and natural gas concentration in the fuel.



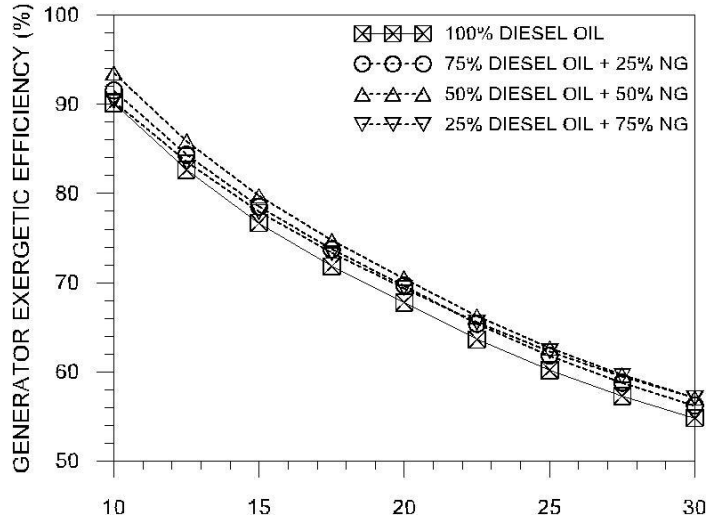
590

591 Figure 5 – Variation of absorption refrigeration system exergetic efficiency with engine

592 load power and natural gas concentration in the fuel.

593

1
2
3
4
5
6
7
8
9
10
11
12
13
14
15
16
17
18
19
20
21
22
23
24
25
26
27
28
29
30
31
32
33
34
35
36
37
38
39
40
41
42
43
44
45
46
47
48
49
50
51
52
53
54
55
56
57
58
59
60
61
62
63
64
65

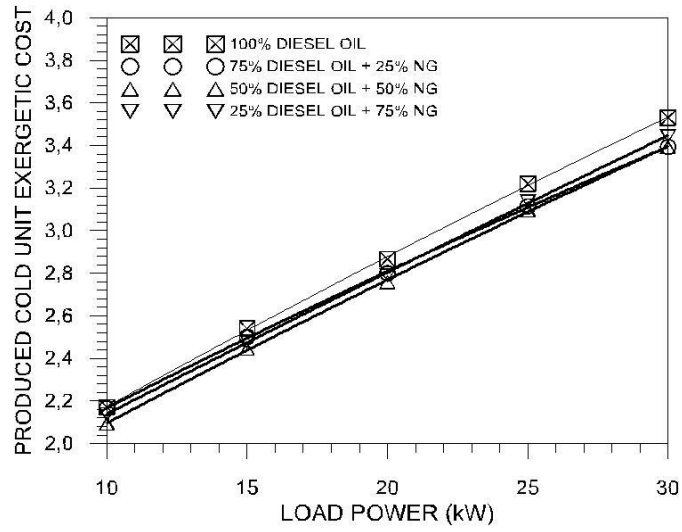


594

595 Figure 6 – Variation of generator exergetic efficiency with engine load power and
596 natural gas concentration in the fuel.

597

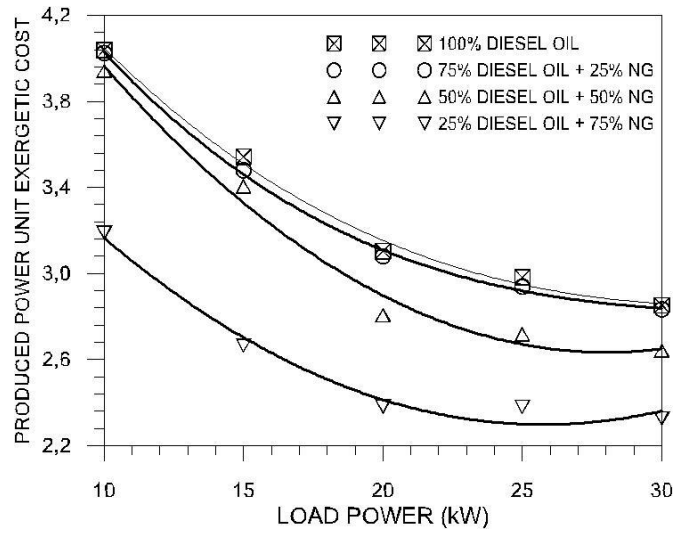
1
2
3
4
5
6
7
8
9
10
11
12
13
14
15
16
17
18
19
20
21
22
23
24
25
26
27
28
29
30
31
32
33
34
35
36
37
38
39
40
41
42
43
44
45
46
47
48
49
50
51
52
53
54
55
56
57
58
59
60
61
62
63
64
65



598

599 Figure 7 – Variation of produced cold unit exergetic cost with engine load power and
600 natural gas concentration in the fuel.

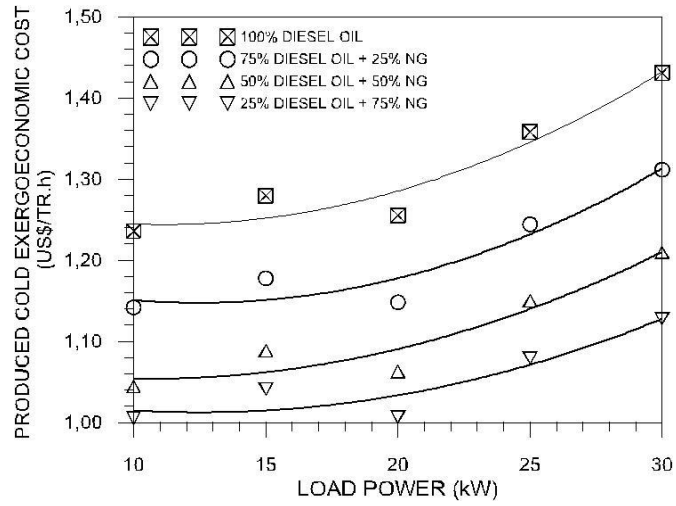
601



602

603 Figure 8 – Variation of produced power unit exergetic cost with engine load power and
 604 natural gas concentration in the fuel.

605

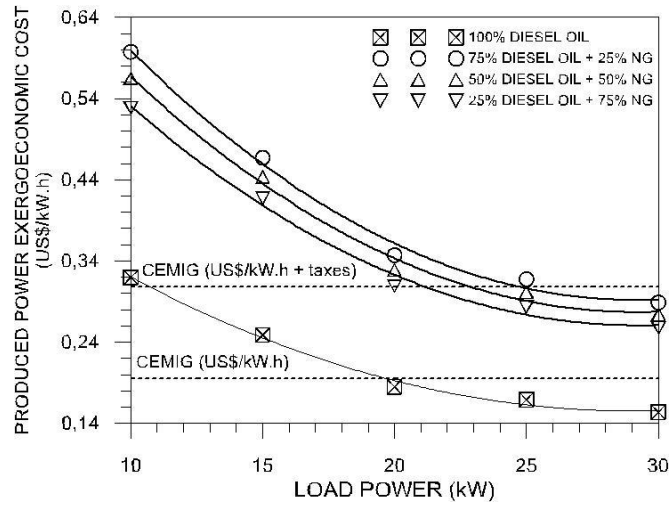


606

607 Figure 9 – Variation of produced cold exergoeconomic cost with engine load power and
 608 natural gas concentration in the fuel.

609

1
2
3
4
5
6
7
8
9
10
11
12
13
14
15
16
17
18
19
20
21
22
23
24
25
26
27
28
29
30
31
32
33
34
35
36
37
38
39
40
41
42
43
44
45
46
47
48
49
50
51
52
53
54
55
56
57
58
59
60
61
62
63
64
65



610

611 Figure 10 – Variation of produced power exergoeconomic cost with engine load power
 612 and natural gas concentration in the fuel.

613